Formation of fullerenes in MeV-ion sputtering from organic solids

G. Brinkmalm, P. Demirev, D. Fenyö, P. Håkansson, J. Kopniczky, and B. U. R. Sundqvist
Division of Ion Physics, Department of Radiation Sciences, Uppsala University, Box 535, S-751 21 Uppsala, Sweden
(Received 22 July 1992)

Even-numbered positive-ion carbon clusters (C_{2n}, $n=20,21,\ldots$) are ejected from a solid film of organic polymer—poly(vinylidene difluoride) (PVDF)—when bombarded by MeV atomic ions. Carbon-cluster ions are formed as a result of a single primary-ion impact. The distribution of cluster sizes suggests that the clusters have closed carbon-cage (fullerene) structure. Measurements of the yield and initial-velocity distributions of the ejected cluster ions are performed in a time-of-flight mass spectrometer equipped with an electrostatic ion mirror. The results are compared to data for ions ejected by MeV projectiles from films of synthetic fullerene (C_{60} and C_{70}) targets. The initial-radial-velocity distribution for cluster ions ejected from the polymer differ markedly from those of synthetic fullerene targets. While C_{60} and C_{70} ions from synthetic fullerene targets have ejection-angle distributions symmetric with respect to the target-surface normal, the mean takeoff angle of carbon-cluster ions ejected from PVDF is off-normal and towards the direction of the incoming primary ion. It is also a clear indication that carbon-cluster ions ejected from PVDF originate in the high-energy-density region created by the fast primary ion. Experiments for establishing the dependence of the carbon-cluster yield Y on the energy loss of the primary ion have been performed. A stronger dependence of the yield for the C_{60} ions desorbed from PVDF targets [$Y \propto (dE/dx)^{3.4}$] than for ions from targets with synthetic C_{60} [$Y \propto (dE/dx)^{2.0}$] has been observed. This supports the conclusion that carbon-cluster ions from PVDF are formed in the axially expanding high-energy-density plasma region.

INTRODUCTION

The existence of a new allotropic form of carbon—closed-shell pure-carbon structures (fullerenes)— was predicted by Kroto *et al.*[1] on the basis of laser-ablation mass-spectrometry results. The C_{60} fullerene structure has been discussed most widely due to the proposal[1] that it has the shape of a truncated icosahedron, consisting of 20 hexagonal and 12 pentagonal faces. The initial observation of fullerenes has been confirmed in a number of papers, reporting the formation of gas-phase carbon-cluster ions with enhanced yield of C_{60} in laser irradiation of graphite and different carbon-containing materials under various experimental conditions.[1-5] It has also been demonstrated that fullerenes can be formed in sooting benzene/oxygen flames.[6] However, the spectacular discovery by Krätschmer *et al.*[7] of a method for synthesis of macroscopic amounts of C_{60} and C_{70} has led to the growth of research on fullerene properties. Fullerenes have already aroused considerable attention among researchers in various fields, including astrophysics, organic chemistry, materials science, and environmental science (for recent comprehensive reviews see Refs. 8 and 9).

In secondary-ion-mass spectrometry (SIMS) studies of different polymeric materials using ^{252}Cf fission fragments with MeV energy to bombard the polymers, Feld *et al.*[10] have observed ejection of even-numbered positive-ion clusters (C_{2n}, $n=20,21,\ldots$) from a specific polymer—poly(vinylidene difluoride) (PVDF), $(-CH_2-CF_2-)_n$. We have expanded these studies[11] by using fast (up to 0.6 MeV/u) atomic ions from the Uppsala EN-tandem accelerator for energy deposition in the PVDF films. The distribution of cluster-yields obtained in this study suggests that stable closed-carbon-cage structures (fullerenes) are formed.[11] The fullerenes are formed as a result of a single MeV-ion impact. Most of the energy of fast MeV ions (with velocities exceeding the Bohr velocity) is deposited in a solid target via ion-electron collisions in an ion track in a time of the order of 10^{-15} s. The track is symmetric around the straight path of the incoming ion. Plasmalike conditions are formed in a cylindrical region roughly 5 Å in diameter where the energy density is greatest. If the relaxation times of the electronic subsystem in the solid are slow, as in the case of insulators, material is sputtered from the solid. This phenomenon is termed electronic sputtering[12] and it has important astrophysical implications.[13] Electronic sputtering is also exploited in a specific version of SIMS—plasma desorption mass spectrometry—and biological macromolecules with molecular weights up to 45 000 u have been ejected from a solid as intact ions into the gas phase with that technique.[14-17] The ejection of positive ions of even-numbered pure-carbon clusters as a result of the interaction of a single fast MeV ion with a polymer containing only 30% carbon atoms is a new specific effect of the electronic-sputtering phenomenon.

In this paper experiments are reported with the aim to elucidate further the mechanism of carbon-cluster formation in electronic sputtering from polymers. For comparison purposes, sputtering induced by MeV atomic ions from targets of C_{60} and C_{70} synthesized according to the method of Krätschmer *et al.*[7] (and henceforth referred to as synthetic fullerene targets) has been also investigated. We have performed experiments on the initial-radial-

 ©1993 The American Physical Society

velocity distribution of carbon clusters of different sizes obtained in electronic sputtering from PVDF. A potential merit of this study is the possibility it affords for determining the origin of the secondary ions relative to the ion track, created by the primary MeV-ion impact.[18–23] Measurements of the initial-axial-velocity distributions have also been performed for carbon clusters ejected from PVDF and synthetic fullerene targets. The axial- and radial-velocity distribution data together provide an estimate of the carbon-cluster-ion takeoff angles, which are compared to the angular distributions of electronically sputtered peptide molecular ions (leu-enkephaline and renin substrate). Experiments on the dependence of the carbon-cluster yield from PVDF and from synthetic fullerene targets on the amount of energy deposited in the solid by the primary MeV ion (the energy loss, dE/dx) have also been carried out.

EXPERIMENT

Instrumental setup and performance

Swift atomic ions were generated in the Uppsala EN-tandem accelerator. A time-of-flight (TOF) mass spectrometer equipped with an electrostatic ion mirror (Fig. 1) was installed on one of the accelerator beam lines (for a detailed description of the construction and performance of the spectrometer see Refs. 23–25). The MeV primary ions passed through a thin (5 $\mu g/cm^2$) carbon foil before reaching the target. Thus the primary ions were in an equilibrium charge state.[26] The secondary electrons emitted from the carbon foil after passage of a single ion were detected by a microchannel plate detector to give the start signal that triggered the timing electronics. The primary MeV ions bombarded the target from the front at an incidence angle of 45°. The target was floated at an acceleration potential $V_a = \pm 14.30$ kV for positive and negative secondary ions, respectively. Desorbed secondary ions were accelerated towards a grid at ground potential through a distance l_a of 4.5 mm. The secondary ions were detected by microchannel plate detectors either in the straight mode (with the electrostatic ion mirror at ground potential) or in the reflected mode (with the mirror at $V_r = \pm 15.66$ kV for positive and negative secondary ions, respectively). The ion-flight-time registration was performed in a pulse-counting mode by employing a multistop (up to 255 stops per start) time-to-digital converter (CTN-M2, IPN, Orsay, France) with 0.5-ns time resolution per channel. Data were acquired in an event-by-event mode at a rate of 10^3 MeV incident ions (events) per second with an ATARI Mega personal computer. Between 1×10^6 and 5×10^6 start events were collected for different experiments depending on the secondary-ion statistics.

Deflection plates (length $l_{dz} = 25$ mm; width $l_{dy} = 16$ mm; distance between them $l_{dx} = 14$ mm) were positioned in the field-free region of the spectrometer at a distance $l_{01} = 166$ mm from the acceleration grid to the front of the x-direction deflection plates (see Fig. 1 for coordinate system assignment). The procedure for measurement of the initial-radial-velocity distribution involved monitoring the secondary-ion yield as a function of electrostatic deflection in an x direction perpendicular to the target-surface normal.[11,20–23] The term "radial velocity" is used throughout the paper for brevity, although only the component of the velocity in the x direction was monitored. The measurements were performed by first maximizing the yield of low-mass ions by setting the potential on the y-deflection plates and then acquiring data for different voltages V_{dx} applied to the x-deflection plates. Conversion from deflection-voltage units to radial-velocity units was performed in a straightforward manner according to

$$v_{0x}^{\text{straight}} = \left[\frac{|q|}{2m}\right]^{1/2} \frac{q}{|q|} \frac{(V_{dx} - V_{0d})}{\sqrt{V_a}} \frac{(l_{dz} + \Delta l_{dz})}{l_{dx}} \times \frac{(\frac{1}{2} l_{dz} + l_{05})}{(2l_a + l_{01} + l_{dz} + l_{05})} \quad (1)$$

when measurements were performed in the straight mode and

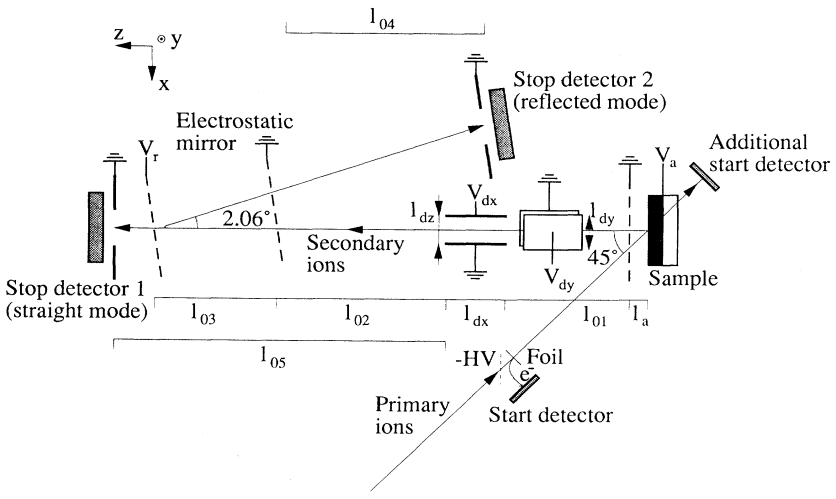

FIG. 1. A schematic of the experimental setup. Distance between target and acceleration grid, $l_a = 4.5$ mm; distance between acceleration grid and x-deflection plates, $l_{01} = 166$ mm; length of the plates, $l_{dz} = 25$ mm; width of the plates, $l_{dy} = 16$ mm; distance between the plates, $l_{dx} = 14$ mm; distance between deflection plates and straight-mode stop detector collimator, $l_{05} = 796$ mm; distance between the plates and reflector grid, $l_{02} = 494$ mm; length of reflector, $l_{03} = 289$ mm; distance between reflector and reflected-mode stop detector collimator, $l_{04} = 435$ mm.

$$v_{0x}^{\text{reflected}} = \left[\frac{|q|}{2m}\right]^{1/2} \frac{q}{|q|} \frac{(V_{dx}-V_{0d})}{\sqrt{V_a}} \frac{(l_{dz}+\Delta l_{dz})}{l_{dx}} \times \frac{\left[\frac{1}{2}l_{dz}+l_{02}+4l_{03}\frac{V_a}{V_r}+l_{04}\right]}{\left[2l_a+l_{01}+l_{dz}+l_{02}+4l_{03}\frac{V_a}{V_r}+l_{04}\right]} \quad (2)$$

in the reflected mode, provided that the energy corresponding to the initial axial velocity of the desorbed ions with mass m and charge q was small compared to the kinetic energy acquired during the acceleration step (i.e., $\frac{1}{2}mv_{0z}^2 \ll qV_a$). The symbols are defined in Fig. 1 and Δl_{dz} (10 mm) is the first-order correction to the length of the finite deflection plates.[20,22,27] A low-mass fragment ion ejected preferentially normal to the target surface[19,22] is used for calculating V_{0d}, the voltage corresponding to zero radial velocity. In the initial-radial-velocity measurements 48-MeV $^{127}I^{10+}$ ions were used as primary ions.

Initial-axial-velocity-distribution measurements were carried out by monitoring the yield for different ions in reflected mode as a function of the ion-reflector potential, while keeping the acceleration potential fixed. This method results only in a relative estimate of the axial velocities for different ions. However, Widdiyasekera *et al.*[28] have performed accurate measurements of the axial velocities of a number of electronically sputtered ions under similar conditions. The values for hydrogen and sodium positive ions determined in these experiments were used as calibrating points for calculation of the axial velocities in our experimental setup. In the initial-axial-velocity measurements 72.3-MeV $^{127}I^{14+}$ ions were used as primary ions.

In the experiments on the secondary-ion-yield dependence on the MeV-ion energy loss in the solid the targets were irradiated with four types of primary ions having the same impact velocity (5 times the Bohr velocity) but different kinetic energies. The primary ions used were 9.9-MeV ^{16}O, 19.7-MeV ^{32}S, 48.6-MeV ^{79}Br, and 78.2-MeV ^{127}I ions. Since the ions had passed through the start detector foil (see above) they were in an equilibrium charge state.[26]

Target preparation

Stainless-steel disks (6 mm in diameter) or square silicon pieces (10×10 mm) were used as backing material for targets in different experiments. We found that the results were not affected by the backing type.

PVDF in powder form was obtained from Aldrich Chemical Co. The PVDF targets were prepared by dissolving the solid polymer in slightly heated acetone (10 $\mu g/\mu l$ concentration) and then spin-coating ~20 μl of the solution on the backing.[29,30] The PVDF target thickness was varied between 100 and 1000 Å by applying different amounts of solution and varying the spinning speed. The film thickness was monitored by ellipsometry.[30]

Synthetic fullerene targets were prepared according to the method of Krätschmer *et al.*[7] The soot was extracted with benzene and the extract was purified by centrifugation. Around 300 μl of the benzene solution was then deposited onto a backing and dried at room temperature, which resulted in a film of C_{60} and C_{70} fullerenes with a thickness of the order of 1 μm.

The peptides leu-enkephaline (555 u) and renin substrate (RS, 1801 u) were obtained from Sigma Chemical Co. The leu-enkephaline target was prepared by dissolving the peptide in a mixture of 80% acetic acid and 20% trifluoro acetic acid (3 $\mu g/\mu l$ concentration) and then electrospraying the solution on a backing. The RS target was prepared by adsorbing the molecules to a thin (a few μm) film of nitrocellulose, formed by electrospraying acetone solution on a backing.[31,32]

RESULTS AND DISCUSSION

Cluster-ion yields

A positive-ion mass spectrum obtained from a synthetic fullerene target bombarded by 72.3-MeV ^{127}I ions is presented in Figs. 2(a) and 2(b). The two major peaks correspond to C_{60}^+ and C_{70}^+ in a ratio of about 2.5 to 1. Higher-mass fullerenes ($m/q > 2000$ a.u.) are also easily identified. This experiment indicates that since electronic sputtering is observed from synthetic fullerene films they are not good electrical conductors under normal conditions. Sputtering after electronic excitation by, e.g., MeV atomic ions, photon, or electrons is effective only if the energy relaxation rate of the electronic subsystem in the solid is low, so that coupling into atomic motion is possible.[12–17] In contrast, material is ejected in the case of nuclear sputtering[12–17] as a result of direct knock-on collisions between incident particles and atoms in the solid. Electronic sputtering yields from conducting materials (e.g., graphite) are, as expected, negligible.[11,33] The total yield (i.e., the number of detected C_{60}^+ and C_{70}^+ per start ion) is about 3%. Negative-ion spectra [Figs. 2(c) and 2(d)] are also easily obtained—the spectra have roughly the same appearance as the positive ones in the region $m/q > 600$ a.u.—including the total yield. Fragmentation and/or neutralization reactions of the ejected ions are also observed. Around 10% of the desorbed positive C_{60}^+ ions decay in the first field-free region (i.e., between the acceleration grid and the reflector) and around 30% of the negative C_{60}^- ions also decay in the same region, as monitored by the straight-mode detector with the ion mirror on and off.

The positive-ion mass spectrum from a PVDF target obtained in the reflected mode is given in Fig. 3. Peaks at regular 24-u intervals are observed from m/q values of 480 to above 4500, which corresponds to clusters around C_{376}. The degrading resolution of the instrument for higher masses due to the lower secondary-ion yield together with the metastable decays is the reason for not extending the range of observed carbon clusters above that mass. No negatively charged carbon clusters from PVDF are observed in this mass range. This fact is an evidence supporting the initial suggestion[11] that carbon-

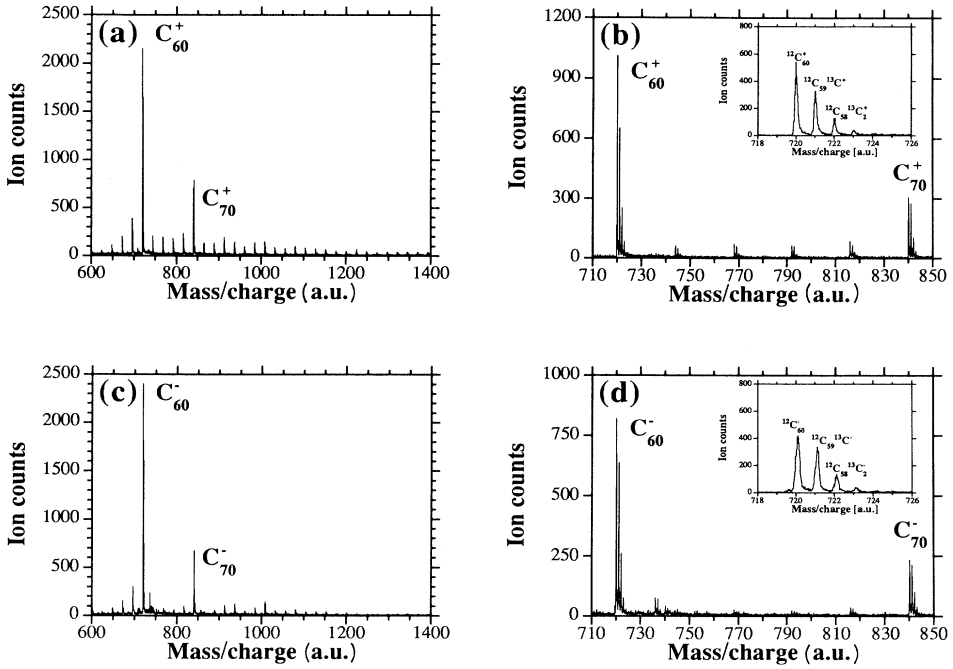

FIG. 2. (a) A time-of-flight (reflected mode) mass spectrum of positive secondary ions from a synthetic fullerene target in the m/q range from 600 to 1400 a.u. (b) Expanded region from the same spectrum in the m/q range from 710 to 850 a.u. The inset shows the resolved peaks for C_{60} due to the natural ^{13}C isotope distribution. (c) A time-of-flight (reflected mode) mass spectrum of negative secondary ions from a synthetic fullerene target in the m/q range from 600 to 1400 a.u. (d) Expanded region from the same spectrum in the m/q range from 710 to 850 a.u. The inset shows the resolved peaks for C_{60} due to the natural ^{13}C isotope distribution.

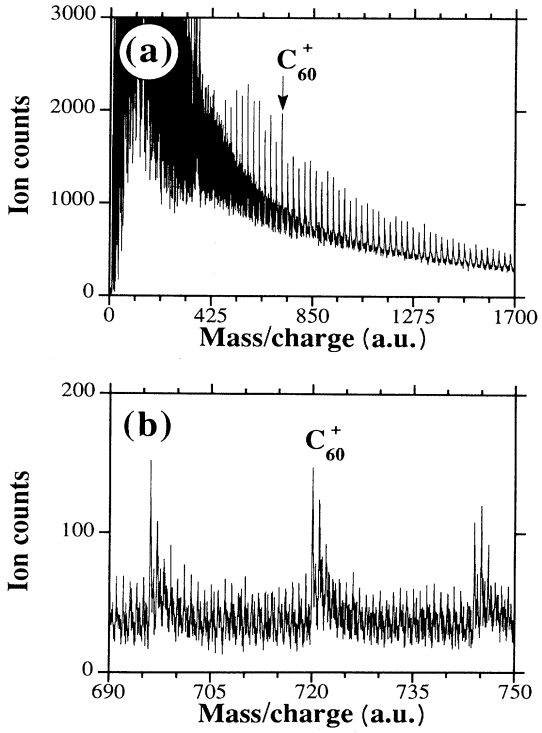

FIG. 3. (a) A time-of-flight (reflected mode) spectrum of positive cluster ions from a PVDF target in the m/q range from 0 to 1700 a.u. (b) Expanded region from the same spectrum in the m/q range from 690 to 750 a.u.

cluster ions originate from the positively charged high-energy-density region. The cluster-ion peaks from PVDF are resolved only in the reflected mode[24] due to their higher initial axial velocity (see below) and metastable decays in the first field-free region of the spectrometer. The isotopic distributions of the cluster ions (C_n, $n=40-110$) as well as accurate determination of their mass show that pure-carbon clusters are detected. As already pointed out,[10,11] PVDF is so far unique as a target material for generation of pure-carbon clusters by MeV-ion bombardment [by contrast no pure-carbon clusters have been observed when Teflon, $(-CF_2-CF_2-)_n$, has been bombarded under the same experimental conditions]. Peaks corresponding to most probably hydrogenated carbon-cluster ions with approximately $2\frac{1}{2}$ times lower intensity than pure-carbon-cluster-ion peaks are present at every integer mass in the spectrum between the even-numbered carbon-cluster peaks (Fig. 3). The carbon clusters are observed instantly when irradiating PVDF targets, i.e., they are formed during the impact of a single primary ion. Thus the assertion that partial carbonization of the polymer is a necessary prerequisite for generation of carbon-cluster ions from PVDF by MeV ions[10] is unfounded. The total yield (i.e., the number of detected pure-carbon cluster per start ion for PVDF) is estimated to be approximately 1%. The carbon-cluster yield as a function of PVDF film thickness increases and saturates at around 300 Å.

Figure 4 shows the even-numbered carbon-cluster-ion yield from PVDF as a function of cluster size (number of

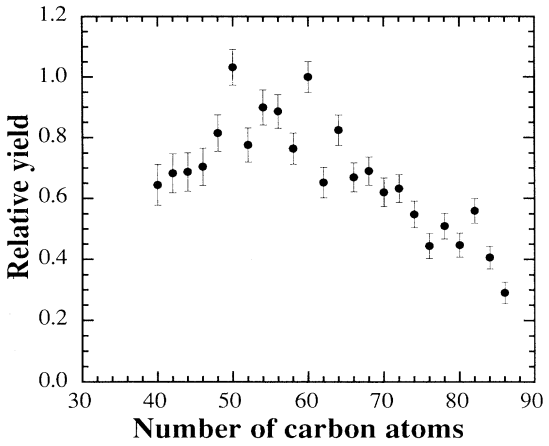

FIG. 4. Yield of carbon-cluster ions desorbed from a PVDF target as a function of number of atoms in the cluster.

carbon atoms in the cluster). A constant background due to the presence of overlapping peaks from hydrogenated cluster ions is subtracted in order to estimate the yield for pure-carbon clusters only. The relative enhancement of the yield for the C_{50} and C_{60} clusters and the corresponding "dips" for the C_{52} and C_{62} clusters are clearly noticeable. The intensity modulation suggests that C_{50} and C_{60} are indeed more stable than the others. This fact as well as the observation of only even-numbered carbon species (starting with clusters containing 40 carbon atoms) strongly indicate that fullerenes are formed in the process. No enhancement of C_{70}, and C_{84} yield is, however, discerned. A plausible explanation connected to the shorter time scale for cluster formation as a result of carbon atom condensation in the dense axially expanding high-energy-density-region plasma may be advanced.[34]

Initial-radial-velocity distributions

Experiments have demonstrated that the initial-radial-velocity distributions of intact peptide ions, sputtered electronically, differ markedly from those of low-mass ions (e.g., CH_3^+).[18–23] This observation, termed directional correlation effect,[20] lends credence to currently accepted models for electronic sputtering,[12,14–17] including the shock wave[35] and pressure pulse[36] models. According to these models the initial radial velocity of the ejected ions depends on their position at the target surface from which they originate, relative to the ion track. High-mass peptide molecular ions are ejected from a lower-energy-density region further away from the ion track core by a radially propagating shock wave (pressure pulse). These ions will accordingly acquire a radial velocity component in a direction off the direction of the incoming MeV ion which is experimentally observed.[18–23] In contrast, low-mass fragment ions (CH_3^+, $C_2H_5^+$, etc.), have an initial-radial-velocity distribution symmetric along the target-surface normal,[19,22] as expected for ions ejected in a thermal evaporation-type process.

In this study we have used an electrostatic-ion-mirror TOF mass spectrometer to estimate the initial-radial-velocity distribution since the electrostatic ion mirror compensates only for the axial-velocity spread thus leaving the radial-velocity component of the secondary ions unaffected.[11,23] An electrostatic-ion-mirror TOF instrument offers also some practical advantages over a conventional linear TOF instrument. These include higher mass resolution, due to axial-velocity focusing and elimination of the neutrals, arising from metastable decays in the first field-free region, and an increase in the signal-to-noise ratio. The yield of different ions ejected from a synthetic fullerene target [Fig. 5(a)] and from a PVDF target [Fig. 5(b)] as a function of deflection voltage demonstrates a striking difference in the initial-radial-velocity distribution of the C_{60}^+ ion in the two experiments. This difference is clearly illustrated in Fig. 6 where the initial-

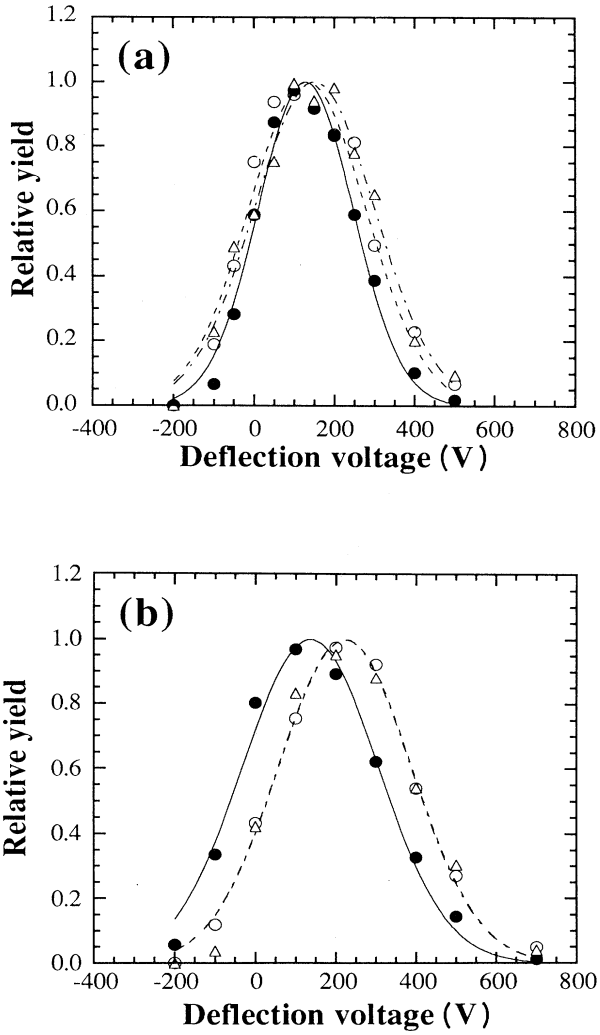

FIG. 5. (a) Yield of $C_2H_3^+$ (●), C_{60}^+, (○), and C_{70}^+ (△) desorbed from a synthetic fullerene target as a function of the voltage V_{dx} between the x-deflection plates. The data points have been fitted to Gaussian curves. (b) Yield of $C_2H_3^+$ (●), C_{60}^+ (○), and C_{70}^+ (△) desorbed from a PVDF target as a function of the voltage V_{dx} between the x-deflection plates. The data points have been fitted to Gaussian curves.

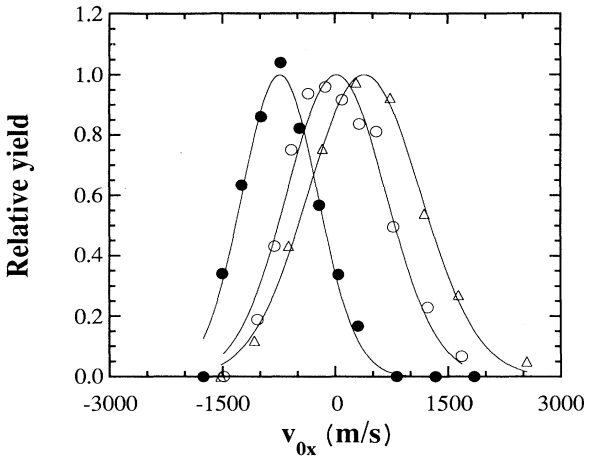

FIG. 6. Initial-radial-velocity distributions for $[M+H]^+$ of leu-enkephaline (●), C_{60}^+ desorbed from fullerene target (○), and C_{60}^+ desorbed from a PVDF target (△). The data points have been fitted to Gaussian curves.

radial-velocity distributions of C_{60}^+ desorbed from a fullerene target and C_{60}^+ desorbed from a PVDF target are plotted together with the distribution of the $[M+H]^+$ ion of the peptide leu-enkephaline. As expected, the initial-radial-velocity distribution of the protonated molecular ion of leu-enkephaline has a maximum in the direction off the direction of the incoming primary-ion beam.[18–23] The rather unexpected observation is that the C_{60}^+ ions from a PVDF target are ejected preferentially backwards along the direction of the incoming MeV ion in a "jet effect" (this term is advanced without any implications of plume formation as in, e.g., laser ablation). To our knowledge, this is the first time such an effect has been encountered in electronic sputtering. The radial-velocity distributions of the other large carbon-cluster ions and the low-mass F^+ and F^{2+} ions (at m/q 19.0 a.u. and 9.5 a.u., respectively) also exhibit shifts in the same direction as the C_{60}^+ ions. This result is in direct contrast to the ejection-angle distributions for the molecular ions of the large organics discussed above. No shift is observed for the C_{60}^+ (and C_{70}^+) carbon-cluster ions compared to the low-mass secondary ions from the synthetic fullerene target (i.e., all these ions are ejected predominantly normal to the surface). The corresponding values for the centroids of the initial-radial-velocity distributions obtained are at +1900 m/s for the F^+ ions from the PVDF target, +400 m/s for the C_{60}^+ ions from the PVDF target, and −800 m/s for the $[M+H]^+$ ion from leu-enkephaline (see Fig. 1 for coordinate system assignment).

The preferentially non-normal ejection of carbon clusters from a PVDF target back along the direction of the incoming primary MeV ion strongly suggests that they are formed at very high energy densities in the high-energy-density plasma and are ejected by the axially expanding track core. Thus a claim by Feld *et al.*[10] that the carbon clusters are formed far out in the ion track at lower energy densities seems not to be valid. The preformed C_{60} ions from synthetic fullerene targets are, in contrast, ejected normally to the target surface, possibly in a thermal evaporation process from the surface region energized by the primary-ion impact.

Initial-axial-velocity distributions

Attempts to measure the initial-axial-velocity distributions for carbon-cluster ions from PVDF and for the molecular ions for RS have been made in order to estimate the ejection-angle distributions for these secondary ions. For comparison the initial axial velocity of C_{60} ions from a synthetic fullerene target has been also measured. The average initial axial velocities obtained are +900 m/s for $[M+H]^+$ of RS, +1200 m/s for synthetic C_{60}^+ ions, and +11 000 m/s for F^+ of PVDF. Thus approximate values of the ejection angles for $[M+H]^+$ of RS and F^+ of PVDF have been determined—the angles between the surface normal and the preferential secondary-ion ejection directions are −30° (away from the primary-ion direction) and +10° (towards the primary-ion direction), respectively. The preformed C_{60}^+ ions, as mentioned above, are ejected normally to the target surface in possibly a thermal evaporation process. Attempts to estimate the initial axial velocity of C_{60}^+ ejected from PVDF were unsuccessful due to interferences from unusually high background caused by metastable decays in the first field-free region. When the mirror voltage is decreased the C_{60}^+ peaks are difficult to discern. Moreover, metastable background peaks begin to dominate since the ion mirror "favors" metastable ion fragments with lower kinetic energies instead of the stable secondary ions. Thus either the method has to be refined (attempts are presently being made) or a different one employed in order to obtain reliable values for the initial axial velocities of the fullerene ions ejected from PVDF.

Energy-density dependence

For a specific target material the radius of the directly ionized and excited region generated by the primary ion as well as the radius and energy-density distribution in the region energized by the secondary electrons is dependent only on the impacting MeV-ion velocity.[33,37] In our experiment MeV primary ions with different energies having the same velocity were used and therefore the ion track size was kept constant. The different primary ions deposit different amounts of energy in the solid and the linear energy-loss values (dE/dx) are estimated by using Bragg's rule and the atomic stopping power values from Ziegler.[38] The dependence of the secondary ion yield on the energy loss for a synthetic fullerene target and for a PVDF target is illustrated in Fig. 7. The ion yield scales as the power of dE/dx. In Table I the values of the power dependence on the energy loss are listed for several different secondary ions. The existence of a threshold value of dE/dx for ejection of carbon clusters from PVDF is established. The threshold values increases with increasing cluster size. The dependence of the yield on the stopping-power for fullerene ions ejected from a PVDF target is unusually high; for comparison we note that the observed stopping-power dependence is of the order of $(dE/dx)^2$ for intact positive biomolecular ions.[39]

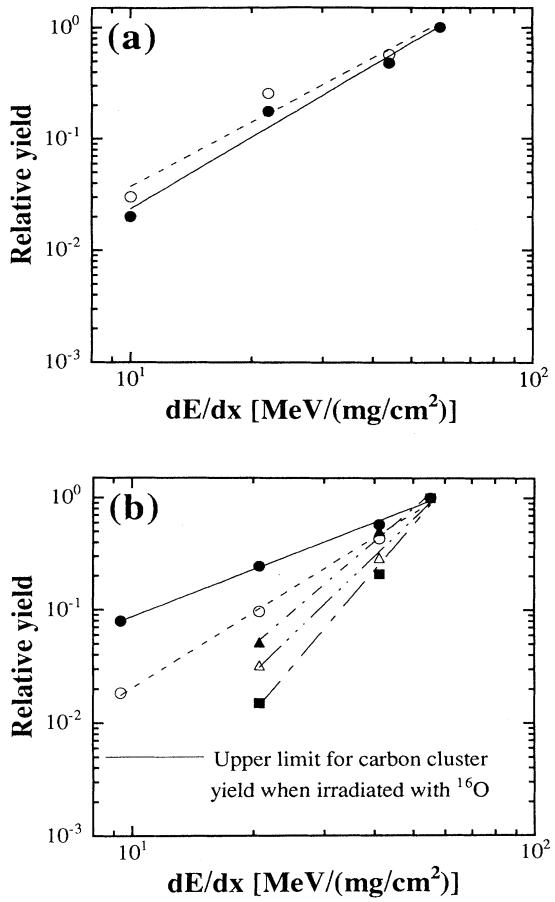

FIG. 7. (a) Yield of $C_2H_3^+$ (●) and C_{60}^+ (○) ejected from a fullerene target as a function of the energy loss of the primary ion in the material. (b) Yield of $C_2H_3^+$ (●), F^+ (○), C_{40}^+ (▲), C_{60}^+ (△), and C_{110}^+ (■) ejected from a PVDF target as a function of the energy loss of the primary ion in the target material.

The stronger dependence of the carbon-cluster yield from a PVDF target on dE/dx supports a model assuming that the clusters originate from the higher-energy-density plasma of the ion track core.[34] In its turn, from the time scales of neutralization and expansion of the high-energy-density region, formation and ejection time of a carbon-cluster ion from a PVDF target of the order of 10^{-12} s may be estimated.[11]

TABLE I. The dependence of the secondary-ion yield on the energy loss [$Y \propto (dE/dx)^n$] for a synthetic fullerene target and for a PVDF target.

Target	Ejected ion	n
Synthetic fullerenes	$C_2H_3^+$	2.3
	C_{60}^+	2.1
PVDF	$C_2H_3^+$	1.4
	F^+	2.2
	F^{2+}	2.2
	C_{40}^+	2.9
	C_{60}^+	3.4
	C_{110}^+	4.1

CONCLUSION

We have demonstrated that fullerenes are formed in MeV-ion bombardment of poly(vinylidene difluoride) polymer on a single-particle-impact basis. Specific aspects of that particular effect of electronic sputtering have been investigated so far. These include the dependence of the fullerene-ion yield on the electronic stopping power of the incident projectile and the initial radial- and axial-velocity distributions of ejected ions. Several new features of the electronic-sputtering phenomenon from PVDF have been encountered. The fullerene-ion yield exhibits an unusually strong (higher than cubic) dependence on the electronic stopping power. Fullerene ions are ejected preferentially back towards the direction of the incoming primary ion in contrast to molecular ions of different biomolecules. Fullerenes are formed by condensation of the atomic carbon vapor in the MeV-ion high-energy-density plasma region, resulting in electronic sputtering of PVDF. The required volume is of the order of 10^4 Å^3, and the process is affected on a subnanosecond time scale. These experimental findings bear implications for the mechanism of fullerene formation in general, giving estimates of the required time frame and spatial domain.

ACKNOWLEDGMENTS

This work was supported by the Swedish Natural Sciences Research Council (NFR) and the Wallenberg Foundation.

[1]H. W. Kroto, J. R. Heath, S. C. O'Brien, R. F. Curl, and R. E. Smalley, Nature **318**, 162 (1985).
[2]H. Kroto, Science **242**, 1139 (1988).
[3]S. C. O'Brien, J. R. Heath, R. F. Curl, and R. E. Smalley, J. Chem. Phys. **88**, 220 (1988).
[4]W. Creasy and J. Brenna, Chem. Phys. **126**, 453 (1988).
[5]W. R. Creasy and J. T. Brenna, J. Chem. Phys. **92**, 2269 (1990).
[6]P. Gerhardt, S. Loffler, and K. Homann, Chem. Phys. Lett. **137**, 306 (1987).
[7]W. Krätschmer, L. D. Lamb, K. Fostiropoulos, and D. R. Huffman, Nature **347**, 354 (1990).
[8]H. Kroto, A. Allaf, and S. Balm, Chem. Rev. **91**, 1213 (1991).
[9]Acc. Chem. Res. **25**(3) (1992).
[10]H. Feld, R. Zurmühlen, A. Leute, and A. Benninghoven, J. Phys. Chem. **94**, 4595 (1990).
[11]G. Brinkmalm, D. Barofsky, P. Demirev, D. Fenyö, P. Håkansson, R. E. Johnson, C. T. Reimann, and B. U. R. Sundqvist, Chem. Phys. Lett. **191**, 345 (1992).
[12]R. E. Johnson and B. U. R. Sundqvist, Phys. Today **45**(3), 28 (1992).
[13]R. E. Johnson, *Energetic Charged-Particle Interactions with Atmospheres and Surfaces* (Springer-Verlag, Berlin, 1990).
[14]B. U. R. Sundqvist, Int. J. Mass Spectrom. Ion Processes **118/119**, 265 (1992).
[15]B. U. R. Sundqvist, Nucl. Instrum. Methods Phys. Res. Sect. B **48**, 517 (1990).

[16]K. Wien, Nucl. Instrum. Methods Phys. Res. Sect. B **65**, 149 (1992).
[17]K. Wien, Radiat. Eff. Defect. Solids **109**, 137 (1989).
[18]W. Ens, B. U. R. Sundqvist, P. Håkansson, D. Fenyö, A. Hedin, and G. Jonsson, J. Phys. (Paris) Colloq. **50**, C2-9 (1989).
[19]R. Moshammer, R. Matthäus, K. Wien, and G. Bolbach, in *Ion Formation from Organic Solids (IFOS V)*, edited by A. Hedin, B. U. R. Sundqvist, and A. Benninghoven (Wiley, Chichester, 1990), p. 17.
[20]W. Ens, B. U. R. Sundqvist, P. Håkansson, A. Hedin, and G. Jonsson, Phys. Rev. B **39**, 763 (1989).
[21]D. Fenyö, A. Hedin, P. Håkansson, R. E. Johnson, and B. U. R. Sundqvist, in *Ion Formation from Organic Solids (IFOS V)* (Ref. 19), p. 33.
[22]D. Fenyö, A. Hedin, P. Håkansson, and B. U. R. Sundqvist, Int. J. Mass Spectrom. Ion Processes **100**, 63 (1990).
[23]P. Demirev, G. Brinkmalm, D. Fenyö, P. Håkansson, and B. U. R. Sundqvist, Int. J. Mass Spectrom. Ion Processes **111**, 41 (1991).
[24]G. Brinkmalm, P. Håkansson, J. Kjellberg, P. Demirev, B. U. R. Sundqvist, and W. Ens, Int. J. Mass Spectrom. Ion Processes **114**, 183 (1992).
[25]G. Brinkmalm, P. Håkansson, J. Kjellberg, and B. U. R. Sundqvist (unpublished).
[26]A. Brunelle, S. Della-Negra, J. Depauw, H. Joret, Y. Le Beyec, and K. Wien, Nucl. Instrum. Methods Phys. Res. Sect. B **43**, 484 (1989).
[27]A. Recknagel, Z. Phys. **111**, 61 (1938).
[28]S. Widdiyasekera, P. Håkansson, and B. U. R. Sundqvist, Nucl. Instrum. Methods Phys. Res. Sect. B **33**, 836 (1988).
[29]G. Säve and B. U. R. Sundqvist, Tandem Accelerator Laboratory (TLU) Report No. 149/87, 1987.
[30]G. Brinkmalm, G. Jonsson, B. U. R. Sundqvist, A. Hedin, and P. Håkansson, in *Ion Formation from Organic Solids (IFOS V)* (Ref. 19), p 55.
[31]G. P. Jonsson, A. B. Hedin, P. L. Håkansson, B. U. R. Sundqvist, B. G. S. Säve, P. F. Nielsen, P. Roepstorff, K.-E. Johansson, I. Kamensky, and M. S. L. Lindberg, Anal. Chem. **58**, 1084 (1986).
[32]G. Jonsson, A. Hedin, P. Håkansson, and B. U. R. Sundqvist, Rapid Commun. Mass Spectrom. **2**, 154 (1988).
[33]W. Brandt and R. H. Ritchie, in *Proceedings, Physical Mechanisms in Radiation Biology,* edited by R. D. Cooper and R. W. Wood (USEC Technical Information Center, Oak Ridge, TN 1974), p. 20.
[34]I. Bitensky *et al.* (unpublished).
[35]I. Bitensky and E. Parilis, Nucl. Instrum. Methods Phys. Res. Sect. B **21**, 26 (1987).
[36]R. E. Johnson, B. U. R. Sundqvist, A. Hedin, and D. Fenyö, Phys. Rev. B **40**, 49 (1989).
[37]A. Hedin, P. Håkansson, B. U. R. Sundqvist, and R. Johnson, Phys. Rev. B **31**, 1780 (1986).
[38]*Handbook of Stopping Cross-sections for Energetic Ions in All Elements,* 1st ed., edited by J. F. Ziegler (Pergamon, New York, 1980).
[39]A. Hedin, P. Håkansson, M. Salehpour, and B. U. R. Sundqvist, Phys. Rev. B **35**, 7377 (1987).